

Relativistic NN scattering without partial wave decomposition

G. Ramalho¹, A. Arriaga^{1,2} and M. T. Peña³

¹Centro de Física Nuclear da Universidade de Lisboa, 1649-003 Lisboa, Portugal

²Departamento de Física, Faculdade de Ciências da Universidade de Lisboa, 1700 Lisboa, Portugal

³Centro de Física das Interações Fundamentais and Department of Physics, Instituto Superior Técnico, Av. Rovisco Pais 1049-001 Lisboa, Portugal

(July 9, 2021)

Abstract

We consider the covariant Spectator equation with a One Boson Exchange (OBE) kernel, and apply it to the NN system. Relativistic effects such as retardation and negative-energy state components are included in that equation. We develop a method, based on the Padé method, to solve the Spectator equation without partial wave decomposition. The convergence of the partial wave decomposition series is tested as a function of the energy. The on- and off-mass-shell amplitudes are calculated. The NN interaction was fitted to the differential cross section for NN scattering, in the energy range below the pion production threshold.

I. INTRODUCTION

Electron scattering experiments off light nuclei at momentum transfer in the few GeV/c region will provide new information on the intermediate and short range behavior of the nuclear interaction [1,2]. In this regime the interpretation of data requires a description based on relativistic kinematics and dynamics, and therefore sets an important challenge to theory. It also raises a technical computational difficulty, since traditional numerical methods to solve dynamical equations are based upon partial wave decomposition (PWD) of the NN interaction. In fact, scattering and bound states are often described by partial waves series. This procedure allows to explore nuclear symmetries and probes expansions in powers of energy/momentum. Moreover, by reducing the dimensionality of the integral equations it saves numerical computational effort, since for low energies (< 200 MeV) the series can be truncated to a few terms. However, for higher energies a large number of partial waves is required and the method becomes unfeasible, specially in applications for nuclear systems with $A > 2$ [3]. In fact two-body scattering amplitudes are input for the three-body amplitudes and, as it is shown in Ref. [4], above 300 MeV the convergence of the series requires more than 15 partial waves. Fortunately, present day computational limitations are not a serious objection anymore to obtaining directly the solution of three-dimensional integral equations without partial wave series.

In short, methods not based on PWD generate numerical problems which are i) straightforward, presenting much less analytical and algebraic complexity than alternative formulations with PWD, ii) usable in the energy region where PWD converge too slowly, and which is probed by the Jlab data for electro- and photo- desintegration of the two- and three-nucleon systems, iii) solvable within reasonable CPU time in present day available computer power.

Since for the energy range mentioned in point ii) relativity becomes also an issue, in this work we develop a method to solve relativistic quasi-potential equations, without PWD, for the NN system, in particular the Spectator equation [5,6] with a realistic NN interaction. The present paper prepares for later applications to photo- and electro- reactions at high energies.

By construction, the Spectator quasi-potential equation incorporates relativistic effects such as retardation and negative-energy state components (ρ -spin states). The focus here is on obtaining a working method to solve it without PWD, proceeding directly through a three-dimensional integration. This is the first work that combines the two aspects, relativity and three-dimensional numerical methods, in a application to the two-nucleon system scattering problem. While we consider here the particular case of the Spectator equation, the method can be extended to other quasi-potential equations. The numerical complexity of the relativistic problem is twice as large as the one of the non-relativistic case. The resulting equation couples 8 channels corresponding to the different final helicities and ρ -spin cases.

In Sec. II an overview of three-dimensional methods and of quasi-potential equations is presented. In Sec. III the detailed presentation of the Spectator equation for fermions is given. The NN interaction is also discussed, as well as the strong form factors required by the stability of the solution. In Sec. IV the method of solving the integral equation without partial wave decomposition is explained. In Sec. V results for NN on-mass-shell amplitudes, NN differential cross section and NN off-mass-shell amplitudes are shown and discussed. Finally, Sec. VII presents the conclusions.

II. BACKGROUND

A. Three-Dimensional (3D) Methods

For energies not larger than 300 MeV, numerical methods without partial wave decomposition, also referred as Three Dimensional (3D) methods [4], were applied to non-relativistic NN scattering with spin and isospin variables, using the Bonn and Argonne interactions. The authors used 2-particle helicity states and the role of the symmetries of the scattering amplitudes in that basis to advantageously reduce the size of the numerical 3D problem.

Importantly, their results showed that in the vicinity of 300 MeV some of those NN amplitudes required already 16 partial waves to converge, making the partial wave method impracticable, specially for use in 3 nucleon calculations. Indeed, in applications to the 3 nucleon system presented on Ref. [3] the PWD method was realized to be inappropriate for 3 nucleon processes at energies higher than 250 MeV. At those energies, both two- and three-nucleon scattering amplitudes were shown to exhibit a strong angular dependence in

the forward and backward scattering angles, preventing an efficient and reasonable description in terms of a few partial waves. Other non-relativistic calculations without partial wave decomposition for the amplitudes of the two- and three- scalar particle systems were published [7,8]. In Ref. [9] relativistic effects of several quasi-potential equations are compared using the 3D method for scalar particles. An advantage of the 3D calculation for scalar particles based on numeric linear system methods is that it works on a relatively large range of energies (300-800 MeV) with, almost, the same number of grid points [7,9].

B. Quasi-Potential (QP) equations

Over the past years different relativistic formulations have been investigated for application to light nuclei, which can be classified in two major categories: Relativistic Hamiltonian Dynamics [10–12] and Relativistic Field Theories [5,13–17]. We will concentrate here on the second ones. They are based on covariant field theories with effective nucleon and meson degrees of freedom. The non-perturbative character of the nuclear interaction definitely requires an infinite sum of meson exchange diagrams, which can be summed effectively by means of integral equations, as the Bethe-Salpeter [13] 4-dimensional equation.

In principle, the kernel of the Bethe-Salpeter equation should include all irreducible diagrams derived from a considered Lagrangian. In practice, models inevitably determine the truncation of the kernel expansion and only a restrict set of appropriate meson exchange diagrams is then kept.

An usual approximation of the Bethe Salpeter equation consists on restricting the integral kernel to a sum of One Boson (Meson) exchange diagrams, which is often called the Ladder Approximation. Nevertheless, this approximation may be questioned. In fact, the one body limit is not recovered when one of the particle masses goes to infinity [5,18]. On the other hand, the crossed-box irreducible diagrams may be important, as confirmed by calculations within the Feynman-Schwinger formalism [19]. Although restricted only to the bound state of scalar particles, Ref. [20] showed that there are some 3-dimensional integral equations that conveniently rearrange the series of ladder and crossed-ladder diagrams, yielding results equivalent to solving the BS equation beyond the ladder approximation. [19]. One of those 3-dimensional integral equations is the Spectator equation.

The quasi-potential (QP) equations are integral equations that are obtained from the Bethe-Salpeter equation through a restriction on the energy variable yielding 3-dimensional integral equations.

In particular, in the Spectator equation this restriction is motivated by important cancellations between box and crossed-box amplitudes. These cancellations are such that their sum reduces to ladder diagrams of the mass pole of the heavier particle or, for equal interacting masses, to ladder diagrams of the mass poles of the two particles. For scalar interacting particles in the one-body limit the above cancellation is exact order by order [5,18]. When one of the masses is much larger than the other, the spectator equation in the ladder approximation alone gives practically the same result as the full Bethe-Salpeter equation, as shown in Ref. [21]. This outcome shows the efficiency gained in the rearrangement of the series. Furthermore, it has been shown that for nucleons (with equal masses) the non-vanishing difference between the sum of box and crossed-box diagrams and the spectator ladder di-

agrams can be effectively represented by one heavier boson exchanges [22]. The Spectator equation, with an appropriate OBE kernel, is therefore suitable for applications to the two- and three-nucleon systems, as successfully done in Refs. [2,6,23,24].

III. SPECTATOR EQUATION FOR FERMIONS

In the original form of the Spectator equation [5] one of the two particles is considered on-mass-shell in the intermediate state. To satisfy the Pauli Principle a new version consisting of a set of two coupled equations was presented in Ref. [6]. Since here we evaluate the scattering amplitude with both particles on-mass-shell in the initial state, the two equations reduce to a single one.

Following Ref. [6] the scattering equation corresponding to the amplitude where particle 1 is on-mass-shell in the initial and final states is written as

$$\begin{aligned} \mathcal{M}_{\alpha'\beta',\alpha\beta}(p',p;P) &= \bar{\mathcal{V}}_{\alpha'\beta',\alpha\beta}(p',p;P) \\ &- \frac{1}{2} \sum_{\alpha_1,\alpha_2} \int \frac{d^3k}{(2\pi)^3} \frac{m}{E_{\mathbf{k}}} \bar{\mathcal{V}}_{\alpha'\beta',\alpha_1\beta_1}(p',k;P) G_{\alpha_1\beta_1,\alpha_2\beta_2}(k;P) \mathcal{M}_{\alpha_2\beta_2,\alpha\beta}(k,p;P), \end{aligned} \quad (3.1)$$

where

$$\bar{\mathcal{V}}_{\alpha'\beta',\alpha\beta}(p',p;P) = \mathcal{V}_{\alpha'\beta',\alpha\beta}(p',p;P) + (-1)^I \mathcal{V}_{\beta'\alpha',\alpha\beta}(-p',p;P), \quad (3.2)$$

is the anti-symmetrized interaction kernel. In the factor $\delta = (-1)^I$ I is the total isospin of the 2-nucleon system. In the notation used m is the nucleon mass, p and p' are the relative initial and final 4-momenta, P the total 4-momentum. Also, the indices that represent the Dirac components of particles 1 and 2 are respectively α' and β' for the final state, and α and β for the initial state. $E_{\mathbf{k}}$ is the on-mass-shell energy corresponding to the three momentum \mathbf{k} : $E_{\mathbf{k}} = \sqrt{m^2 + \mathbf{k}^2}$. We considered the c.m. reference frame where $P = (W, 0)$ (W is the total energy). When both particles are on-mass-shell the relative 3-momentum is represented by $\bar{\mathbf{p}}$ and then $W = 2E_{\bar{\mathbf{p}}}$.

In Eq. (3.1) $G_{\alpha_1\beta_1,\alpha_2\beta_2}(k;P)$ is the 2-nucleon Spectator propagator given by

$$G_{\alpha_1\beta_1,\alpha_2\beta_2}(k;P) = \Lambda_{\alpha_1\alpha_2}(P/2 + k) G_{\beta_1\beta_2}(P/2 - k), \quad (3.3)$$

where $\Lambda_{\alpha_1\alpha_2}(k_1)$ is the particle 1 positive-energy projector and $G_{\beta_1\beta_2}(k_2)$ the particle 2 Dirac propagator. In Eq. (3.1) the asymmetry due to the propagator G is only apparent, since the anti-symmetrization is implemented by means of the kernel in Eq. (3.2).

To write the scattering amplitude in terms of the helicity and ρ -spin we perform the change of basis similar to the one of the Ref. [6]:

$$\begin{aligned} \mathcal{M}_{\lambda'_1\lambda'_2,\lambda_1\lambda_2}^{\rho'_1\rho'_2,\rho_1\rho_2}(p',p;P) &= \\ \sum_{\alpha',\beta'} \bar{u}_{1\alpha'}^{\rho'_1}(p',\lambda'_1) \bar{u}_{2\beta'}^{\rho'_2}(p',\lambda'_2) \mathcal{M}_{\alpha'\beta',\alpha\beta}(p',p;P) u_{1\alpha}^{\rho_1}(p,\lambda_1) u_{2\beta}^{\rho_2}(p,\lambda_2), \\ &\alpha,\beta \end{aligned} \quad (3.4)$$

where u_j^\pm with $j = 1, 2$ are the asymptotic states of the particles (see Appendix A), λ_1 (λ'_1) and λ_2 (λ'_2) are the initial (final) helicities respectively for particles 1 and 2. The indices ρ_j and ρ'_j with $j = 1, 2$ express the initial and final ρ -spin states for particle j . A similar expression holds for \mathcal{V} .

The scattering amplitude in terms of the helicity and ρ -spin reads:

$$\begin{aligned} \mathcal{M}_{\lambda'_1 \lambda'_2, \lambda_1 \lambda_2}^{+\rho'_2, +\rho_2}(p', p; P) &= \bar{\mathcal{V}}_{\lambda'_1 \lambda'_2, \lambda_1 \lambda_2}^{+\rho'_2, +\rho_2}(p', p; P) \\ &- \sum_{\rho, \lambda_3, \lambda_4} \int \frac{d^3 k}{(2\pi)^3} \bar{\mathcal{V}}_{\lambda'_1 \lambda'_2, \lambda_3 \lambda_4}^{+\rho'_2, +\rho}(p', k; P) g^\rho(k; W) \mathcal{M}_{\lambda_3 \lambda_4, \lambda_1 \lambda_2}^{+\rho, +\rho_2}(k, p; P), \end{aligned} \quad (3.5)$$

where

$$g^+(k; W) = \frac{1}{2} \left(\frac{m}{E_{\mathbf{k}}} \right)^2 \frac{1}{2E_{\mathbf{k}} - W - i\varepsilon} \quad (3.6)$$

$$g^-(k; W) = -\frac{1}{2} \left(\frac{m}{E_{\mathbf{k}}} \right)^2 \frac{1}{W}. \quad (3.7)$$

Note that in the Spectator formalism one of the particles is always on-mass-shell in a positive-energy state and that is why in Eq. (3.5) there is always a positive ρ -spin state in the initial, intermediate and final states. The diagrammatic representation of the Eq. (3.5) is given in the Fig. 1. The crosses on the lines mean that the corresponding particles are on mass-shell with positive energy.

The kernel $\bar{\mathcal{V}}$ contains two terms, the direct term and the exchange term (see Eq. (3.2)), which are represented in Fig. 2. In this work we use an OBE kernel including π , σ , ρ and ω meson exchanges. For π exchange we consider a mixture of pseudo-scalar (PS) and pseudo-vector (PV) couplings, defined as:

$$\Lambda_\pi(p', k) = \lambda_\pi \gamma^5 + (1 - \lambda_\pi) \frac{(\not{p}' - \not{k})}{2m} \gamma^5, \quad (3.8)$$

where $0 \leq \lambda_\pi \leq 1$ is the admixture parameter.

The kernel parameters are presented in table I along with the cut-off parameters of the form factors (see Sec. III C). The m_π , m_ρ and m_ω parameters are fixed by the experimental values for physical mesons. The remaining 11 parameters were fitted to NN scattering data. We may anticipate at this point that the best results obtained favor the PV coupling ($\lambda_\pi = 0$). The model used for the kernel is very similar to the one of the Refs. [6,23]. Explicit expressions for \mathcal{V} can be found in Appendix B.

A. Prescription for the Exchange Kernel

For the direct term the 4-momentum transfer q is given by

$$q^2 = (p'_1 - k_1)^2 \quad (3.9)$$

while for the exchange term by

$$\hat{q}^2 = (p'_1 - k_2)^2. \quad (3.10)$$

The relation of these four-momenta with the relative four-momenta is given by

$$p'_1 = (E_{\mathbf{p}'}, \mathbf{p}') \quad (3.11)$$

$$p'_2 = (W - E_{\mathbf{p}'}, -\mathbf{p}') \quad (3.12)$$

$$k_1 = (E_{\mathbf{k}}, \mathbf{k}) \quad (3.13)$$

$$k_2 = (W - E_{\mathbf{k}}, -\mathbf{k}). \quad (3.14)$$

When particle 1 is on-mass-shell with positive-energy the momentum transfer reads:

$$-q^2 = (\mathbf{p}' - \mathbf{k})^2 - (E_{\mathbf{p}'} - E_{\mathbf{k}})^2 \quad (3.15)$$

$$-\hat{q}^2 = (\mathbf{p}' + \mathbf{k})^2 - (E_{\mathbf{p}'} + E_{\mathbf{k}} - W)^2, \quad (3.16)$$

respectively for the direct and exchange terms of the kernel (see Fig. 2). We may then conclude that, while the direct term has no singularities in the meson propagators (we have always $\mu^2 - q^2 > 0$), the exchange term may have the singularity corresponding to an on-mass-shell exchanged meson ($\mu^2 = \hat{q}^2$). The condition $\mu^2 = \hat{q}^2$ indicates a real meson production from off-mass-shell nucleon states. However, since a real meson production process is not allowed below the pion production threshold, the singularity of $\hat{\mathcal{V}}$ has no physical correspondence. It is simply a consequence of the anti-symmetrization of the kernel (see Eq.(3.2)). As shown by Gross *et al* this spurious singularity is cancelled by higher order diagrams [6].

In the numerical applications of the Spectator equations two prescriptions were considered so far to deal with the spurious singularities [6]:

- the "principal part prescription": the singularity is included but only the Principal Part of the integral is kept. This corresponds to the replacement

$$\int \frac{1}{\mu^2 - \hat{q}^2 - i\varepsilon} \rightarrow \mathcal{P} \int \frac{1}{\mu^2 - \hat{q}^2} = \int \left(\frac{1}{\mu^2 - \hat{q}^2 - i\varepsilon} - i\pi\delta(\mu^2 - \hat{q}^2) \right).$$

- the "energy independent prescription": the momentum transfer is modified in order to remove the singularity. This amounts to the replacement

$$\hat{q} = p'_1 - k_2 \rightarrow q = p'_1 - k_1,$$

that is, the momentum transfer is the same for the propagator in both direct and exchange diagrams, leaving the meson propagator denominator independent of the two-nucleon system energy W (see Eq. (3.15)).

We now introduce the on-shell prescription, an alternative adopted by us in the present work.

Eq. (3.16) can be rewritten as follows:

$$-\hat{q}^2 = (\mathbf{p}' + \mathbf{k})^2 - (E_{\mathbf{p}'} - E_{\mathbf{k}})^2 - (W - 2E_{\mathbf{p}'})(W - 2E_{\mathbf{k}}). \quad (3.17)$$

The last term of this equation generates the spurious singularities mentioned above, and vanishes when both particles are on-mass-shell either in the initial state ($W = 2E_{\mathbf{k}}$) or in

the final state ($W = 2E_{\mathbf{p}'}$). We therefore define the “on-mass-shell prescription”, by taking for $-\hat{q}^2$ the expression

$$-\hat{q}^2 \rightarrow (\mathbf{p}' + \mathbf{k})^2 - (E_{\mathbf{p}'} - E_{\mathbf{k}})^2. \quad (3.18)$$

With this choice the exchange kernel $\hat{\mathcal{V}}$ is consistent with the Feynman rules in the on-mass-shell limit. This is a physical argument in favor of the proposed prescription. Furthermore, the plus sign in Eq. (3.18) implies that when the direct term in a particular interaction is dominant in the forward direction, then the exchange term dominates in the backward direction, as it happens for interactions mediated by scalars. We point out that this property is not satisfied by the “energy independent prescription”, where the exchange kernel \hat{q} is replaced by the direct kernel momentum q . Note also that the “on-mass-shell prescription” is energy independent.

B. Properties and Symmetries of the Amplitudes

Using parity, time reversal and particle interchange symmetries we can decrease the number of independent amplitudes [25,26]. In particular, parity invariance reduces the 16 helicity amplitudes with $\rho' = +1$, $\rho = +1$ states to 8 independent ones, according to:

$$M_1 = \mathcal{M}_{++,++}(\mathbf{p}', u; \mathbf{p}, 1) = \mathcal{M}_{--,--}(\mathbf{p}', u; \mathbf{p}, 1) \quad (3.19)$$

$$M_2 = \mathcal{M}_{--,++}(\mathbf{p}', u; \mathbf{p}, 1) = \mathcal{M}_{++,--}(\mathbf{p}', u; \mathbf{p}, 1) \quad (3.20)$$

$$M_3 = \mathcal{M}_{+-,+-}(\mathbf{p}', u; \mathbf{p}, 1) = \mathcal{M}_{-+,-+}(\mathbf{p}', u; \mathbf{p}, 1) \quad (3.21)$$

$$M_4 = \mathcal{M}_{-+,-+}(\mathbf{p}', u; \mathbf{p}, 1) = \mathcal{M}_{+-,+-}(\mathbf{p}', u; \mathbf{p}, 1) \quad (3.22)$$

$$M_5 = \mathcal{M}_{-+,++}(\mathbf{p}', u; \mathbf{p}, 1) = -\mathcal{M}_{+-,--}(\mathbf{p}', u; \mathbf{p}, 1) \quad (3.23)$$

$$M_6 = \mathcal{M}_{+-,++}(\mathbf{p}', u; \mathbf{p}, 1) = -\mathcal{M}_{-+,--}(\mathbf{p}', u; \mathbf{p}, 1) \quad (3.24)$$

$$M_7 = \mathcal{M}_{++,+-}(\mathbf{p}', u; \mathbf{p}, 1) = -\mathcal{M}_{--,+-}(\mathbf{p}', u; \mathbf{p}, 1) \quad (3.25)$$

$$M_8 = \mathcal{M}_{--,+-}(\mathbf{p}', u; \mathbf{p}, 1) = -\mathcal{M}_{++,+-}(\mathbf{p}', u; \mathbf{p}, 1). \quad (3.26)$$

In the case $\rho' = -1$ the right hand side should include the phase $(-1)^{\frac{1-\rho'}{2}} = -1$.

The above relations are valid either \mathbf{p}' is on- or off-mass-shell. Restricting to the on-mass-shell situation, further relations arise:

$$M_7 = M_6 \quad (3.27)$$

$$M_8 = -M_5 \quad (3.28)$$

$$M_5 = -M_6. \quad (3.29)$$

The last identity is valid only for identical particles (exact isospin symmetry). As a result we are left with only 5 independent amplitudes. We point out that these relations are independent of the interaction used and of any prescription adopted, and are merely a result of the symmetries mentioned above. The relations (3.19)-(3.26) were tested numerically as a check to the code, since we did not explicitly impose the symmetries to reduce the number of equations.

If we consider instead a QP equation of the instantaneous type (no retardation), e.g. the Blankenbecler-Sugar [14] or the Equal-Time [15] equations, where the particles have always the same energy, we could use more symmetry properties to reduce further the number of off-mass-shell amplitudes.

Finally we note that, for equations of the instantaneous type, a convenient combination of the helicity states defines states of well defined parity and two-body spin and helicity. The use of that basis states reduces the size of the numerical problem by block-diagonalizing the set of equations. This was done for example in Ref. [3,4] in a non-relativistic framework (no $\rho' = -1$ states). Nevertheless, for 3-body applications [3] the helicity combination has to be inverted by calculating back the amplitudes in the asymptotic basis of uncoupled helicities.

C. Strong Form Factors

Nucleons are not elementary particles and their hadronic structure has to be taken into account through form factors. Mathematically, such form factors provide the necessary regularization of the integrals for the high order loops. Since in this work we solve the scattering equation without partial wave expansion, a careful study of the integrand function had to be performed in order to determine form factor functions adequate for the convergence of the method used.

The starting point for the choice of form factors was the decomposition suggested by Riska and Gross [27]

$$F_i(p'_j, k_j) = f_{m_i}(q^2) f_N(p_j'^2) f_N(k_j^2), \quad (3.30)$$

where p'_j (k_j) is the final (initial) momentum of the nucleon j , $q = p'_j - k_j$ is the transfer momentum, f_{m_i} is the form factor of meson i and f_N the nucleon form factor. This factorization is adequate to describe the electromagnetic interaction with nucleons, and the scalar functions f_N and f_m could be interpreted as strong interaction vertex corrections and self-energy contributions of nucleons and mesons. As shown in Ref. [22], however, some care has to be taken in the functional forms of the form factors considered in the above prescription. In fact, the most used momentum dependence of f_N [6,23] induces additional spurious singularities in a 4-dimensional framework, which can be eliminated by distorting conveniently the contour for energy integration around them [28]. These spurious singularities, however, do not occur within a QP context.

For the meson form factor our choice is

$$f_{m_i}(q^2) = \frac{\Lambda_{m_i}^2}{\Lambda_{m_i}^2 - q^2}, \quad (3.31)$$

where Λ_{m_i} is the cut off of meson i . Note however, that by construction the functions $f_{m_i}(q^2)$ only modify the kernel for large q^2 (for $q^2 = 0$ we have $f_{m_i}(q^2) = 1$), and do not suppress the large momentum dependence of $\mathcal{V}(k, k; P)$.

For the f_N form factors we take

$$f_N(k_j^2) = \left[\frac{\tilde{\Lambda}_N^2}{\tilde{\Lambda}_N^2 + (m^2 - k_j^2)^2} \right]^n, \quad (3.32)$$

with

$$\tilde{\Lambda}_N^2 = \Lambda_N^2 - m^2. \quad (3.33)$$

being Λ_N the nucleon cut-off. The f_N functions regulate the asymptotic behavior of both $\mathcal{V}(k, k; P)$ and $\mathcal{V}(k, p; P)$. The factorization (3.30) has been applied by Gross and collaborators in several applications of the Spectator equation [6,23]. The function (3.32) with $n = 1$ has been used for the first time in Ref. [23] and kept in Spectator equation applications since then. The meson form factor used in the same applications differs from (3.31) for large q^2 . The factorization (3.30) with the presented f_m and f_N ($n = 1$) functional forms has been also used in Ref. [29], but in an instantaneous quasi-potential framework (where $k = (0, \mathbf{k})$). In the present calculation we found that in order to solve the Spectator equation with 3D methods the value $n = 1$, used in previous applications with PWD, was not large enough to allow the convergence of $\mathcal{M}(k, p; P)$ for large $|\mathbf{k}|$. We had to take instead $n = 2$. This is mostly due to the meson propagator behavior which peaks for forward and backward scattering angles at high values of the momentum [30]. Using the PWD method the meson propagator peak is smeared by the angle integration, but in the 3D method the structure of the propagator cannot be smoothened.

IV. SOLUTION OF THE INTEGRAL EQUATION WITHOUT PARTIAL WAVE DECOMPOSITION

In order to solve the scattering equation analytical or numerically we need to specify the scattering conditions, that is the initial and final momenta. We choose a reference frame where the incoming momentum is along the z axis and express the initial, final and intermediate momenta in terms of spherical coordinates

$$\mathbf{p} = (p, 0, 0) \quad (4.1)$$

$$\mathbf{p}' = (p', \theta', \varphi') \quad (4.2)$$

$$\mathbf{k} = (k, \theta, \varphi). \quad (4.3)$$

where $p' = |\mathbf{p}'|$, $p = |\mathbf{p}|$ and $k = |\mathbf{k}|$.

A. Integration of the Azimuthal Angle

To perform the φ integration we need to apply on the scattering amplitude a rotation of an angle φ around the z axis. In Appendix C we show that:

$$\mathcal{M}_{\lambda_3 \lambda_4, \lambda_1 \lambda_2}^{+ \rho'_{2,+} \rho_2}(\mathbf{k}, \theta, \varphi; \mathbf{p}; W) = e^{i(\lambda_1 - \lambda_2) \frac{\varphi}{2}} \mathcal{M}_{\lambda_3 \lambda_4, \lambda_1 \lambda_2}^{+ \rho'_{2,+} \rho_2}(\mathbf{k}, \theta, 0; \mathbf{p}; W), \quad (4.4)$$

where the \mathbf{p} angles are omitted by simplicity.

Inserting Eq. (4.4) in the Spectator Eq. (3.5), and taking $\varphi' = 0$, we can factorize the φ dependence obtaining

$$\begin{aligned} \mathcal{M}_{\lambda'_1 \lambda'_2, \lambda_1 \lambda_2}^{+\rho'_2, +\rho_2}(p', \theta', 0; p; W) &= \bar{\mathcal{V}}_{\lambda'_1 \lambda'_2, \lambda_1 \lambda_2}^{+\rho'_2, +\rho_2}(p', \theta', 0; p; W) \\ &- \sum_{\rho, \lambda_3, \lambda_4} \int \frac{k^2 dk}{2\pi} \int \frac{d \cos \theta}{2\pi} V_{\lambda'_1 \lambda'_2, \lambda_3 \lambda_4}^{+\rho'_2, +\rho}(p', \theta', k, \theta; \bar{\lambda}, W) g^\rho(k; W) \mathcal{M}_{\lambda_3 \lambda_4, \lambda_1 \lambda_2}^{+\rho, +\rho_2}(k, \theta, 0; p; W), \end{aligned} \quad (4.5)$$

where

$$V_{\lambda'_1 \lambda'_2, \lambda_3 \lambda_4}^{+\rho'_2, +\rho}(p', \theta', k, \theta; \bar{\lambda}, W) = \frac{1}{2\pi} \int d\varphi e^{i\bar{\lambda}\varphi} \bar{\mathcal{V}}_{\lambda'_1 \lambda'_2, \lambda_3 \lambda_4}^{+\rho'_2, +\rho}(p', \theta', \varphi'; k, \theta, \varphi; W), \quad (4.6)$$

and

$$\bar{\lambda} = \frac{\lambda_1 - \lambda_2}{2} \quad (4.7)$$

can take the values $0, \pm 1$.

The scattering equation, Eq. (4.5), is now in 2-dimensional form and includes the propagator function $g^\rho(k; W)$ which has a real pole at $k = \bar{p}$ ($W = 2E_{\mathbf{k}}$) for $\rho = +1$. Performing the contour integration we obtain

$$\begin{aligned} \mathcal{M}_{\lambda'_1 \lambda'_2, \lambda_1 \lambda_2}^{+\rho'_2, +\rho_2}(p', \theta', 0; p; W) &= \bar{\mathcal{V}}_{\lambda'_1 \lambda'_2, \lambda_1 \lambda_2}^{+\rho'_2, +\rho_2}(p', \theta', 0; p; W) \\ &- \sum_{\rho, \lambda_3, \lambda_4} \mathcal{P} \int \frac{k^2 dk}{2\pi} \int \frac{d \cos \theta}{2\pi} V_{\lambda'_1 \lambda'_2, \lambda_3 \lambda_4}^{+\rho'_2, +\rho}(p', \theta'; k, \theta; \bar{\lambda}, W) g_{\varepsilon=0}^\rho(k; W) \mathcal{M}_{\lambda_3 \lambda_4, \lambda_1 \lambda_2}^{+\rho, +\rho_2}(k, \theta, 0; p; W) \\ &- i \frac{m^2 \bar{p}}{4W} \sum_{\lambda_3, \lambda_4} \int \frac{d \cos \theta}{2\pi} V_{\lambda'_1 \lambda'_2, \lambda_3 \lambda_4}^{+\rho'_2, ++}(p', \theta'; \bar{p}, \theta; \bar{\lambda}, W) \mathcal{M}_{\lambda_3 \lambda_4, \lambda_1 \lambda_2}^{++, +\rho_2}(\bar{p}, \theta, 0; p; W). \end{aligned} \quad (4.8)$$

In this equation we use $g_{\varepsilon=0}^\rho(k; W)$ to represent the $\varepsilon = 0$ limit of $g^\rho(k; W)$ (see Eqs. (3.6)-(3.7)). The multiplicative factor of the last term is a result of the residue

$$\frac{1}{2} \left[\frac{1}{2} \left(\frac{m}{E_{\mathbf{k}}} \right)^2 \frac{k^2}{\left| \frac{d}{dk} (2E_{\mathbf{k}} - W) \right|} \right]_{k=\bar{p}} = \frac{m^2 \bar{p}}{4W}. \quad (4.9)$$

In Eq. (4.8) only the function $g^+(k; W)$ has a singularity but we include the principal part symbol \mathcal{P} also for $\rho = -1$ for the sake of simplicity.

The φ -integration (4.6) can be performed either analytical or numerically. In Refs. [3,4,7-9] the numerical integration was made. Here we choose the analytical integration in order to minimize computing time. The complexity of the analytical expressions depends crucially upon the f_m form factors. Relatively simple results are obtained for the monopolar choice (3.31). In this case we can write Eq. (4.6) as

$$\int d\varphi e^{i\bar{\lambda}\varphi} \bar{\mathcal{V}}_{\lambda'_1 \lambda'_2, \lambda_3 \lambda_4}^{+\rho'_2, +\rho_2}(p', p; P) = \sum_{\Gamma} C_{\Gamma} \int d\varphi \frac{e^{i\Gamma\varphi}}{(a - b \cos \varphi)(c - b \cos \varphi)^2}, \quad (4.10)$$

where $\Gamma = 0, \pm 1, \pm 2$, and C_{Γ} is a known function of the momentum magnitudes and polar angle. Any term of the last equation is subsequently easily integrated over. Meanwhile, in Ref. [31], where the equation for π -N scattering is solved also without PWD, the authors came also to the same analytical technique but for an integrand not including form factors. Details of the analytical structure of the kernel can be found in Appendix B and the main steps for the analytical integration are given in Appendix D.

B. Numerical Method: Padé Method

The relevant variables in the scattering equation (4.8) may be emphasized by the following convenient change of notation: we denote each of the eight possible helicity and ρ -spin combinations by a single index $I' = \{\rho'_2, \lambda'_1, \lambda'_2\}$, $I_k = \{\rho, \lambda_3, \lambda_4\}$ and $I_0 = \{\rho_2, \lambda_1, \lambda_2\}$, according to table II (I' , I_k and I_0 have nothing to do with the total isospin I); we omit the total energy W , incoming momentum p and total isospin I dependences and perform the following substitutions

$$\begin{aligned}\mathcal{M}_{\lambda'_1\lambda'_2,\lambda_1\lambda_2}^{+\rho'_2,+\rho_2}(p', \theta', 0; p; W) &\rightarrow \mathcal{M}_{I',I_0}(p', u) \\ \bar{\mathcal{V}}_{\lambda'_1\lambda'_2,\lambda_1\lambda_2}^{+\rho'_2,+\rho_2}(p', \theta', 0; p; W) &\rightarrow \bar{\mathcal{V}}_{I',I_0}(p', u) \\ V_{\lambda'_1\lambda'_2,\lambda_3\lambda_4}^{+\rho'_2,+\rho}(p', \theta'; k, \theta; \bar{\lambda}, W) &\rightarrow V_{I',I_k}(p', u; k, v),\end{aligned}$$

where

$$u = \cos \theta' \quad (4.11)$$

$$v = \cos \theta. \quad (4.12)$$

Finally Eq. (4.8) simplifies to

$$\begin{aligned}\mathcal{M}_{I',I_0}(p', u) &= \bar{\mathcal{V}}_{I',I_0}(p', u) \\ &- \sum_{I_k=1}^8 \mathcal{P} \int_0^\infty \frac{k^2 dk}{2\pi} \int_{-1}^1 \frac{dv}{2\pi} V_{I',I_k}(p', u; k, v) g^{I_k}(k; W) \mathcal{M}_{I_k,I_0}(k, v) \\ &- i \frac{m^2 \bar{\mathcal{P}}}{4W} \sum_{I_k=1}^4 \int_{-1}^1 \frac{dv}{2\pi} V_{I',I_k}(p', u; \bar{\mathcal{P}}, v) \mathcal{M}_{I_k,I_0}(\bar{\mathcal{P}}, v),\end{aligned} \quad (4.13)$$

with

$$g^{I_k}(k; W) = \begin{cases} g_{\varepsilon=0}^+(k; W) & \text{if } I_k = 1, \dots, 4 \\ g^-(k; W) & \text{if } I_k = 5, \dots, 8 \end{cases}. \quad (4.14)$$

In order to obtain a numerical solution of Eq. (4.13) we carry out a discretization of the integral variables, $k \in [0, +\infty[$ and $v \in [-1, 1]$, and use a gaussian quadrature integration technique. We choose a grid of $N_p + 1$ points for all momenta, p' , k and p , and a grid of $N_u + 1$ points for the angular variables u and v . With this discretization procedure we transform the integral equation (4.8) into an algebraic set of equations:

$$M = V + C \cdot M, \quad (4.15)$$

where M and V are the matrix vectors $\mathcal{M}_{I',I_0}(k_{i'}, v_{j'})$ and $\mathcal{V}_{I',I_0}(k_{i'}, v_{j'})$. The C matrix can be decomposed as $C = A + B$. For $I_k = 1, \dots, 4$, we have

$$A_{(I' i' j'), (I_k i j)} = -\frac{w'_i h_j}{(2\pi)^2} k_i^2 V_{I',I_k}(k_{i'}, u_{j'}; k_i, u_j) g^+(k_i; W) \quad (4.16)$$

$$B_{(I' i' j'), (I_k i j)} = -\frac{h_j}{(2\pi)^2} \frac{m^2 \bar{\mathcal{P}}}{2} \left(i \frac{\pi}{W} - \Delta S \right) V_{I',I_k}(k_{i'}, u_{j'}; \bar{\mathcal{P}}, u_j) \delta_{i, N_p+1} \quad (4.17)$$

with

$$\Delta S = S - S' \quad (4.18)$$

$$S = \mathcal{P} \int_0^{+\infty} dk \frac{k}{E_{\mathbf{k}}^2} \frac{1}{2E_{\mathbf{k}} - W} = -\frac{1}{W} \log \frac{W - 2m}{2m} \quad (4.19)$$

$$S' = \sum_{i=1}^{N_p} w'_i \frac{k_i}{E_{k_i}^2} \frac{1}{2E_{k_i} - W}. \quad (4.20)$$

For $I_k = 5, \dots, 8$, we have

$$A_{(I'ij'), (I_kij)} = -\frac{w'_i h_j}{(2\pi)^2} k_i^2 V_{I', I_k}(k_{i'}, u_{j'}; k_i, u_j) g^-(k_i; W) \quad (4.21)$$

$$B_{(I'ij'), (I_kij)} = 0. \quad (4.22)$$

In the previous equations w'_i and h_j are respectively the gaussian weights for the variables k_i and u_j . The momentum grid is obtained from a $x_i \in]0, 1[$ grid by a change of variable

$$k_i = \Lambda \frac{x_i}{1 - x_i},$$

where typically we take $\Lambda \simeq 0.5 m$. In order to determine the on-mass-shell forward scattering amplitude we add the points $k_{N_p+1} = \bar{p}$ and $u_{N_u+1} = 1$ with zero weight.

The dimension of the above matrices is $n = 8(N_p + 1)(N_u + 1)$, which is a large number when N_p and N_u are of the order of 20. Therefore, a standard matrix inversion method requiring a large computer memory (for double precision complex numbers), becomes impracticable. To overcome this limitation we use instead the Padé method, which gives a fast estimate of the result of the Born series for the coupled set of equations

$$M = \lambda V + \lambda C \cdot M, \quad (4.23)$$

where the λ parameter is introduced by convenience and set to 1 at the end of the calculation. The usual power expansion for $2N + 1$ terms reads

$$M = \lambda M^{(1)} + \lambda^2 M^{(2)} + \lambda^3 M^{(3)} + \dots + \lambda^{2N+1} M^{(2N+1)}. \quad (4.24)$$

The $M^{(i)}$ vectors are evaluated by

$$M^{(1)} = V \quad (4.25)$$

$$M^{(i+1)} = C \cdot M^{(i)}. \quad (4.26)$$

and any element m of the M vector given by

$$m = \lambda m_1 + \lambda^2 m_2 + \lambda^3 m_3 + \dots + \lambda^{2N+1} m_{2N+1}, \quad (4.27)$$

is approximated by a rational function of λ

$$m_{\text{Padé}}(\lambda) = \lambda \frac{a_0 + \lambda a_1 + \dots + \lambda^N a_N}{1 + \lambda b_1 + \dots + \lambda^N b_N}, \quad (4.28)$$

where the $2N + 1$ a_l and b_l coefficients are determined through the $2N + 1$ m_l coefficients, after equating Eqs. (4.27) and (4.28). This method is known in the literature as SPA (Scalar Padé Approximant) [32] and $m_{\text{Padé}}$ denotes the Padé[N, N] result.

The advantage of the Padé method is that it replaces the matrix inversion by a fast estimate of the Born expansion, where all terms are evaluated as a matrix-vector multiplication. This multiplication can be performed as n dot-products of two vectors of n dimension. Therefore the calculation requires memory to allocate only $2n$, instead of n^2 , complex numbers. This reduces substantially the dimension of the problem. The price to pay is the recalculation of the matrix lines.

As we will see in the following section, 11 to 15 Padé terms are needed for convergence. The full calculation takes 1h to 2h CPU time in a Pentium IV at 3GHz. The memory size required is 50 MB.

V. RESULTS AND DISCUSSION

In this section we discuss the results obtained for the on- and off-mass-shell amplitudes, the fit to the np differential cross section, and the convergence of the amplitude as a function of the energy.

The numerical results were checked to satisfy the Optical Theorem:

$$\text{Im}[\mathcal{M}_{\lambda_1\lambda_2,\lambda_1\lambda_2}^{++,++}(\bar{\mathbf{p}}, 1; \bar{\mathbf{p}}, 1)] = -\frac{m^2\bar{\mathbf{p}}}{4W} \sum_{\lambda_3\lambda_4} \int_{-1}^1 \frac{dv}{2\pi} |\mathcal{M}_{\lambda_3\lambda_4,\lambda_1\lambda_2}^{++,++}(\bar{\mathbf{p}}, v; \bar{\mathbf{p}}, 1)|^2. \quad (5.1)$$

Since the optical theorem only probes the on-mass-shell amplitudes, the results for the off-mass-shell amplitudes were tested by numerically checking that they satisfy the symmetry properties as described in Section IIIB.

A. On-mass-shell Amplitudes and Differential Cross Section

Asymptotically the state of the two nucleons is characterized by the individual isospin states. Therefore, for the np system, we must consider

$$T_{\lambda'_1\lambda'_2,\lambda_1\lambda_2}^{np}(\mathbf{p}', u; \mathbf{p}, 1) = \frac{1}{2}T_{\lambda'_1\lambda'_2,\lambda_1\lambda_2}^{10}(\mathbf{p}', u; \mathbf{p}, 1) + \frac{1}{2}T_{\lambda'_1\lambda'_2,\lambda_1\lambda_2}^{00}(\mathbf{p}', u; \mathbf{p}, 1), \quad (5.2)$$

where $T_{\lambda'_1\lambda'_2,\lambda_1\lambda_2}^{I0}$ represents the anti-symmetrized matrix \mathcal{M} with a total isospin I ($I_z = 0$).

Figs. 3 and 4 show the scattering amplitudes (both real and imaginary parts) obtained, at a fixed energy $T_{lab} = 300$ MeV, for all independent helicity channels. The comparison between the exact result and the PWD results with increasing values of the total angular momentum J is shown.

The convergence of the Padé amplitudes has been carefully examined, and the iteration procedure stopped when both real and imaginary parts of T converge with a relative error lower than 10^{-2} . We conclude that in general grids with $N_p = 20$ $N_u = 30$ were enough for the numerical convergence of the solution, although $N_p = N_u = 20$ were sufficient below 200 MeV.

For the helicity $\lambda_1\lambda_2 = +-$ channel convergence requires 13 Padé terms for $I = 0$ and 11 terms for $I = 1$. For the $\lambda_1\lambda_2 = ++$ channel 15 terms for $I = 0$ and 13 terms for $I = 1$ are necessary. In all cases optical theorem has always satisfied with a relative error smaller than 10^{-2} .

After calculating all the on-mass-shell polarized amplitudes we can evaluate the differential cross section

$$\frac{d\sigma}{d\Omega}(\bar{\mathbf{p}}, u) = \frac{1}{(2\pi)^2} \frac{m^4}{W^2} |\overline{T^{np}(\bar{\mathbf{p}}, u)}|^2. \quad (5.3)$$

In this equation $|\overline{T^{np}}|^2$ is given by

$$|\overline{T^{np}(\bar{\mathbf{p}}, u)}|^2 = \frac{1}{4} \sum_{\substack{\lambda'_1, \lambda'_2 \\ \lambda_1, \lambda_2}} |T_{\lambda'_1\lambda'_2, \lambda_1\lambda_2}^{np}(\bar{\mathbf{p}}, u; \bar{\mathbf{p}}, 1)|^2, \quad (5.4)$$

which corresponds to an average over the initial helicity states and a sum of the final ones. In Fig. 10 the fit of the NN potential model to the differential cross section np data at energies $T_{lab}=99, 200$ and 319 MeV is shown. Data are collected from the Nijmegen data-basis [33] and correspond to Refs. [34–36].

At least for the two first energies the quality of the fit is very good. The $T_{lab} = 319$ MeV energy case is already very near the pion production threshold, which justifies the slight decrease of the quality of the fit. Nevertheless, we conclude from this fit that the method developed in the present work is reliable and promising. Another point worth mentioning is that the fit selects the PV pion-nucleon coupling (mixing parameter $\lambda_\pi = 0$), in agreement with requirements from chiral symmetry.

B. Off-mass-shell Amplitudes

The off-mass-shell $T_{\lambda'_1\lambda'_2, \lambda_1\lambda_2}^{np}(\mathbf{p}', u; \bar{\mathbf{p}}, 1)$ amplitudes may be plotted as functions of 2 variables in momentum space.

The results for the 8 $\rho' = +1$ amplitudes are presented in Figs. 6 and 7 for $T_{lab} = 300$ MeV. The $\rho' = -1$ amplitudes plots are presented in Figs. 8 and 9. Note that the on-mass-shell region corresponds to the line $p' = 0.375$ GeV.

It is interesting to note that the off-mass-shell region is very important for all channels. In fact the magnitudes of some amplitudes are important up to momenta of the order 1.5 GeV, much larger than the on-mass-shell momentum. It is also important to point out that the amplitudes involving transitions to negative-energy states, $\rho' = -1$, have magnitudes of the same order of the $\rho' = +1$ amplitudes. Therefore, degrees of freedom corresponding to negative-energy states may have considerable weight within covariant effective field theories. Consequently, although explicitly absent in non relativistic models, they are accounted for in an effective way through the fitting procedures yielding low energy non relativistic realistic potentials.

VI. BREAKING OF PWD FOR HIGH ENERGIES

We present here the study of the PWD convergence as a function of the energy. To perform this decomposition we follow Ref. [26]. Figure 10 shows the convergence of the PWD to the full calculation for a particular neutron-proton on-mass-shell T matrix, for three energy cases. We notice here that the imaginary part of T converges faster than the real part. For each energy case the criterium for convergence was defined as a deviation less than 1% from the full result.

We can see in the Fig. 10 that for 200 MeV more that 10 partial waves are needed to achieve convergence. We confirmed that some helicity channels at 300 MeV require 16 partial waves, as obtained in the non-relativistic calculation of Ref. [4]. As mentioned before, this large number of partial waves makes the PWD method impracticable to generate the two-body amplitudes required as an input for the three-body bound or scattering calculation as seen in Ref. [3] within a non relativistic framework.

On the other hand, the results for 100 MeV show that it is a good approximation at low energies to take $J = 6$ as the highest total angular momentum. This explicit finding fully justifies the cut-off at $J = 6$ reported in the three-body bound state relativistic calculations of Ref. [23].

VII. CONCLUSIONS

We considered the Spectator equation for nucleons. Its solution depends on the helicities of the particles, as well as on their ρ -spins. ($\rho' = +1$ for the positive-energy state component and $\rho' = -1$ for the negative-energy state component).

The scattering amplitude is solved without partial wave decomposition using the Padé method. This method revealed to be efficient and suitable for the solution of the relativistic integral equation without partial wave decomposition. For $T_{lab} < 350$ MeV, from 11 to 15 Padé terms were needed for convergence.

Strong form factors and a prescription for the exchange kernel different from the ones considered in other calculations within the spectator formalism are used. When both particles are on-mass-shell the present prescription for the exchange kernel gives rise to the kernel directly obtained from the Feynman rules. This is important in view of possible applications to problems where the fields are not effective, the $q\bar{q}$ bound state and the quark exchange diagrams in $\pi\pi$ scattering.

We fitted an OBE interaction to the differential np differential cross section in the 100-350 MeV energy range. We let the percentage of PS and PV admixture to float as a free parameter of the fit. It turned out that the PV coupling was favored by the fit, which is in agreement arguments of chiral symmetry.

We studied the convergence of the PWD method as a function of the energy. We concluded that above $T_{lab} = 250$ MeV at least 16 partial waves have to be included for some helicity cases. This large number of terms indicates the breaking of the PWD method for applications in heavier nuclei.

Beyond the $\rho' = +1$ amplitudes involved in the cross section calculation, we have also calculated the $\rho' = -1$ amplitudes related to processes involving one off-mass-shell particle.

These amplitudes are numerically significant and may be used in the calculation of meson production cross sections [37,38] and of the $^3\text{He}(e, e')X$ reaction observables for 1-10 GeV energies [1].

ACKNOWLEDGMENTS

This work was performed partially under the grant PRAXIS XXI BD/9450/96 and grant POCT/FNU/50358/2002. One of the authors (G. R.) would like to thank Alfred Stadler for helpful discussions. M. T. P. and G. R. thank Franz Gross and Charlotte Elster for discussions, and the Jefferson Laboratory Theory group for the hospitality during their visit.

APPENDIX A: STATES OF HELICITIES

1. Positive-energy state spinors

Following the construction of Refs. [39,40] we obtain for the spinors the expressions:

$$u_j(\mathbf{k}, \lambda) = N_k \begin{bmatrix} 1 \\ \lambda \tilde{k} \end{bmatrix} |\lambda >_j, \quad (\text{A1})$$

with the normalization

$$N_k = \sqrt{\frac{m + E_{\mathbf{k}}}{2m}} \quad (\text{A2})$$

$$\tilde{k} = \frac{k}{m + E_{\mathbf{k}}}. \quad (\text{A3})$$

The Pauli spinors of the particle 1 and 2

$$|\lambda >_1 = \chi_{\lambda}(\hat{\mathbf{k}}) \quad (\text{A4})$$

$$|\lambda >_2 = \psi_{\lambda}(\hat{\mathbf{k}}). \quad (\text{A5})$$

are related by

$$\psi_{\lambda}(\hat{\mathbf{k}}) = \chi_{-\lambda}(\hat{\mathbf{k}}). \quad (\text{A6})$$

Initial and final state Pauli spinors are presented in table III.

2. Negative-energy spinor states

The negative-energy spinors are constructed from positive-energy states using the charge conjugation operator C [6,39,40]:

$$v_1(\mathbf{k}, \lambda) = (-1)\lambda C \bar{u}_2^T(\mathbf{k}, \lambda) \quad (\text{A7})$$

$$v_2(\mathbf{k}, \lambda) = \lambda C \bar{u}_1^T(\mathbf{k}, \lambda), \quad (\text{A8})$$

where $C = -i\gamma^0\gamma^2$ and T indicates matrix transposition. The relative factors are introduced by convenience. As a result we get

$$v_i(\mathbf{k}, \lambda) = N_k \begin{bmatrix} -\lambda\tilde{k} \\ 1 \end{bmatrix} |\lambda >_i. \quad (\text{A9})$$

APPENDIX B: KERNEL $\bar{\mathcal{V}}$

In this Appendix we describe the analytical structure of the kernel with the OBE form. As mentioned before, for any isospin state I , the kernel $\bar{\mathcal{V}}$ contains the direct, \mathcal{V} , term and the exchange kernel, $\hat{\mathcal{V}}$, term:

$$\bar{\mathcal{V}}_{\lambda'_1\lambda'_2,\lambda_1\lambda_2}^{+\rho',+\rho}(p', k; P) = \mathcal{V}_{\lambda'_1\lambda'_2,\lambda_1\lambda_2}^{+\rho',+\rho}(p', k; P) + (-1)^I \hat{\mathcal{V}}_{\lambda'_1\lambda'_2,\lambda_1\lambda_2}^{+\rho',+\rho}(p', k; P). \quad (\text{B1})$$

For meson i the direct term is given by

$$\begin{aligned} \mathcal{V}_{\lambda'_1\lambda'_2,\lambda_1\lambda_2}^{+\rho',+\rho}(p', k; P) &= \delta_I \frac{g_i^2}{\mu_i^2 - q^2} \bar{u}^+(p'_1, \lambda'_1) \Lambda_1(p'_1, k_1) u^+(k_1, \lambda_1) \\ &\quad \bar{u}^{\rho'}(p'_2, \lambda'_2) \Lambda_2(p'_2, k_2) u^\rho(k_2, \lambda_2) [f_{m_i}(q^2)]^2 f_N(p'^2_2) f_N(k^2_2). \end{aligned} \quad (\text{B2})$$

where the exchange momentum is

$$q^2 = (E_{\mathbf{p}'} - E_{\mathbf{k}})^2 - (\mathbf{p}' - \mathbf{k})^2. \quad (\text{B3})$$

For vector mesons we have to undertake the substitution

$$\Lambda_1 \Lambda_2 \rightarrow \Lambda_1^\mu(p'_1, k_1) \Lambda_2^\nu(p'_2, k_2) \left[g_{\mu\nu} + \frac{(p'_1 - k_1)_\mu (p'_2 - k_2)_\nu}{\mu_i^2} \right]. \quad (\text{B4})$$

Similarly for the exchange term we have

$$\begin{aligned} \hat{\mathcal{V}}_{\lambda'_1\lambda'_2,\lambda_1\lambda_2}^{+\rho',+\rho}(p', k; P) &= \delta_I \frac{g_i^2}{\mu_i^2 - \hat{q}^2} \bar{u}^+(p'_1, \lambda'_1) \Lambda_1(p'_1, k_2) u^\rho(k_2, \lambda_2) \\ &\quad \bar{u}^{\rho'}(p'_2, \lambda'_2) \Lambda_2(p'_2, k_1) u^+(k_1, \lambda_1) [f_{m_i}(\hat{q}^2)]^2 f_N(p'^2_2) f_N(k^2_2), \end{aligned} \quad (\text{B5})$$

where, according to the "on-mass-shell prescription" the exchange momentum is

$$\hat{q}^2 = (E_{\mathbf{p}'} - E_{\mathbf{k}})^2 - (\mathbf{p}' + \mathbf{k})^2. \quad (\text{B6})$$

For vector mesons the replacement is now

$$\Lambda_1 \Lambda_2 \rightarrow \Lambda_1^\mu(p'_1, k_2) \Lambda_2^\nu(p'_2, k_1) \left[g_{\mu\nu} + \frac{(p'_1 - k_2)_\mu (p'_2 - k_1)_\nu}{\mu_i^2} \right]. \quad (\text{B7})$$

The calculation results are presented in Sec. B 1 for the direct term and Sec. B 2 for the exchange term. For the sake of simplicity we do not explicit the parameters involved but only the analytical structure.

1. Direct Kernel

We will write the direct kernel by means of the following auxiliary functions

$$Z_1^0(\hat{\mathbf{p}}', \hat{\mathbf{k}}) = \chi_{\lambda_1'}^\dagger(\hat{\mathbf{p}}') \chi_{\lambda_1}(\hat{\mathbf{k}}) \quad (\text{B8})$$

$$Z_2^0(\hat{\mathbf{p}}', \hat{\mathbf{k}}) = \psi_{\lambda_2'}^\dagger(\hat{\mathbf{p}}') \psi_{\lambda_2}(\hat{\mathbf{k}}), \quad (\text{B9})$$

$$Z_1^i(\hat{\mathbf{p}}', \hat{\mathbf{k}}) = \chi_{\lambda_1'}^\dagger(\hat{\mathbf{p}}') \sigma_i^{(1)} \chi_{\lambda_1}(\hat{\mathbf{k}}) \quad (\text{B10})$$

$$Z_2^i(\hat{\mathbf{p}}', \hat{\mathbf{k}}) = \psi_{\lambda_2'}^\dagger(\hat{\mathbf{p}}') \sigma_i^{(2)} \psi_{\lambda_2}(\hat{\mathbf{k}}) \quad (\text{B11})$$

The Z_j^α functions ($j = 1, 2$, $\alpha = 0, \dots, 3$) are calculated from the Pauli spinors presented in Appendix A. For simplicity sometimes we suppress the arguments of Z_j^α .

a. Meson σ

$$\begin{aligned} \mathcal{V}_{\lambda_1' \lambda_2', \lambda_1 \lambda_2}^{+ \rho', + \rho}(p', k) &= -\frac{g_\sigma^2}{\mu_\sigma^2 - q^2} [f_\sigma(q^2)]^2 f_N(p'^2) f_N(k^2) \\ &\quad N_{p'}^2 N_k^2 H_\sigma(p', k) \\ &\quad Z_1^0(\hat{\mathbf{p}}', \hat{\mathbf{k}}) Z_2^0(\hat{\mathbf{p}}', \hat{\mathbf{k}}) \end{aligned} \quad (\text{B12})$$

$H_\sigma(p', k)$ is also a function of λ_1' , λ_2' , λ_1 , λ_2 , ρ' and ρ .

For large k we have $H_\sigma(p', k) \sim 1$.

b. Meson π

$$\begin{aligned} \mathcal{V}_{\lambda_1' \lambda_2', \lambda_1 \lambda_2}^{+ \rho', + \rho}(p', k; P) &= \delta_I \frac{g_\pi^2}{\mu_\pi^2 - q^2} [f_\pi(q^2)]^2 f_N(p'^2) f_N(k^2) \\ &\quad N_{p'}^2 N_k^2 H_\pi(p', k) \\ &\quad Z_1^0(\hat{\mathbf{p}}', \hat{\mathbf{k}}) Z_2^0(\hat{\mathbf{p}}', \hat{\mathbf{k}}) \end{aligned} \quad (\text{B13})$$

$H_\pi(p', k)$ is also a function of λ_1' , λ_2' , λ_1 , λ_2 , ρ' and ρ .

For large k we have $H_\pi(p', k) \sim 1$ for PS coupling and $H_\pi(p', k) \sim k/m$ for PV coupling.

c. Vector mesons

$$\begin{aligned} \mathcal{V}_{\lambda_1' \lambda_2', \lambda_1 \lambda_2}^{+ \rho', + \rho}(p', k; P) &= \delta_I \frac{g_v^2}{\mu_v^2 - q^2} [f_v(q^2)]^2 f_N(p'^2) f_N(k^2) \\ &\quad N_{p'}^2 N_k^2 H_v(p', k). \end{aligned} \quad (\text{B14})$$

$$\begin{aligned} H_v(p', k) &= r_0 Z_1^0 Z_2^0 + r_1 \sum_{i=1}^3 Z_1^i Z_2^i + r_2 \sum_{i=1}^3 (p'_i + k_i) Z_1^0 Z_2^i \\ &\quad + r_3 \sum_{i=1}^3 (p'_i + k_i) Z_1^i Z_2^0 + r_4 \sum_{i=1}^3 (p'_i + k_i)^2 Z_1^0 Z_2^0. \end{aligned} \quad (\text{B15})$$

The coefficients r_l ($l = 0, \dots, 4$) are functions of the momenta \mathbf{p}' , \mathbf{k} , of the indices λ'_1 , λ'_2 , λ_1 , λ_2 , ρ' , ρ and of the κ_v parameter.

For large \mathbf{k} we have $H_v(p', k) \sim 1$ when $\kappa_v = 0$ and $H_v(k, k) \sim k^2/m^2$ and $H_v(p', k) \sim k/m$ when $\kappa_v \neq 0$.

2. Exchange Kernel

For the exchange term we use the auxiliary functions

$$\hat{Z}_1^0(\hat{\mathbf{p}}', \hat{\mathbf{k}}) = \chi_{\lambda'_1}^{\prime\dagger}(\hat{\mathbf{p}}') \psi_{\lambda_2}(\hat{\mathbf{k}}) \quad (\text{B16})$$

$$\hat{Z}_2^0(\hat{\mathbf{p}}', \hat{\mathbf{k}}) = \psi_{\lambda'_1}^{\prime\dagger}(\hat{\mathbf{p}}') \chi_{\lambda_1}(\hat{\mathbf{k}}), \quad (\text{B17})$$

$$\hat{Z}_1^i(\hat{\mathbf{p}}', \hat{\mathbf{k}}) = \chi_{\lambda'_1}^{\prime\dagger}(\hat{\mathbf{p}}') \sigma_i^{(1)} \psi_{\lambda_2}(\hat{\mathbf{k}}) \quad (\text{B18})$$

$$\hat{Z}_2^i(\hat{\mathbf{p}}', \hat{\mathbf{k}}) = \psi_{\lambda'_2}^{\prime\dagger}(\hat{\mathbf{p}}') \sigma_i^{(2)} \chi_{\lambda_1}(\hat{\mathbf{k}}). \quad (\text{B19})$$

These functions are also evaluated from the Pauli spinors.

a. Meson σ

$$\begin{aligned} \hat{\mathcal{V}}_{\lambda'_1 \lambda'_2, \lambda_1 \lambda_2}^{+\rho', +\rho}(p', k; P) &= -\frac{g_\sigma^2}{\mu_\sigma^2 - \hat{q}^2} [f_\sigma(\hat{q}^2)]^2 f_N(p'^2) f_N(k^2) \\ &\quad N_{p'}^2 N_k^2 \hat{H}_\sigma(p', k) \\ &\quad \hat{Z}_1^0(\hat{\mathbf{p}}', \hat{\mathbf{k}}) \hat{Z}_2^0(\hat{\mathbf{p}}', \hat{\mathbf{k}}) \end{aligned} \quad (\text{B20})$$

$\hat{H}_\sigma(p', k)$ is also a function of λ'_1 , λ'_2 , λ_1 , λ_2 , ρ' and ρ .

For large \mathbf{k} we have $\hat{H}_\sigma(p', k) \sim 1$.

b. Meson π

$$\begin{aligned} \hat{\mathcal{V}}_{\lambda'_1 \lambda'_2, \lambda_1 \lambda_2}^{+\rho', +\rho}(p', k; P) &= \delta_I \frac{g_\pi^2}{\mu_\pi^2 - q^2} [f_\pi(q^2)]^2 f_N(p'^2) f_N(k^2) \\ &\quad N_{p'}^2 N_k^2 \hat{H}_\pi(p', k) \\ &\quad \hat{Z}_1^0(\hat{\mathbf{p}}', \hat{\mathbf{k}}) \hat{Z}_2^0(\hat{\mathbf{p}}', \hat{\mathbf{k}}) \end{aligned} \quad (\text{B21})$$

$\hat{H}_\pi(p', k)$ is also a function of λ'_1 , λ'_2 , λ_1 , λ_2 , ρ' and ρ .

For large \mathbf{k} we have $\hat{H}_\pi(p', k) \sim 1$ for PS coupling and $\hat{H}_\pi(p', k) \sim k/m$ and $\hat{H}_\pi(k, k) \sim k^2/m^2$ for PV coupling.

c. Vector mesons

$$\widehat{\mathcal{V}}_{\lambda'_1 \lambda'_2, \lambda_1 \lambda_2}^{+, \rho', + \rho}(p', k; P) = \delta_I \frac{g_v^2}{\mu_v^2 - q^2} [F_v(q^2)]^2 N_{p'}^2 N_k^2 \widehat{H}_v(p', k). \quad (\text{B22})$$

$$\begin{aligned} \widehat{H}_v(p', k) = & r_0 \widehat{Z}_1^0 \widehat{Z}_2^0 + r_1 \sum_{i=1}^3 \widehat{Z}_1^i \widehat{Z}_2^i + r_2 \sum_{i=1}^3 (p'_i - k_i) \widehat{Z}_1^0 \widehat{Z}_2^i \\ & + r_3 \sum_{i=1}^3 (p'_i - k_i) \widehat{Z}_1^i \widehat{Z}_2^0 + r_4 \sum_{i=1}^3 (p'_i - k_i)^2 \widehat{Z}_1^0 \widehat{Z}_2^0. \end{aligned} \quad (\text{B23})$$

The coefficients r_l ($l = 0, \dots, 4$) are a function the momenta p' , k , of λ'_1 , λ'_2 , λ_1 , λ_2 , ρ' , ρ and also of the κ_v parameter. The r_l coefficients for the exchange kernel are not related with the direct kernel coefficients.

For large k we have $\widehat{H}_v(p', k) \sim 1$ when $\kappa_v = 0$ and $\widehat{H}_v(k, k) \sim k^2/m^2$ and $\widehat{H}_v(p', k) \sim k/m$ when $\kappa_v \neq 0$.

APPENDIX C: φ ROTATED AMPLITUDE

In this appendix we derive the relation between the scattering amplitude on the scattering plane (\mathbf{p} is on the z axis)

$$\mathcal{M}_{\lambda'_1 \lambda'_2, \lambda_1 \lambda_2}^{+, \rho'_2, + \rho_2}(p', \theta', 0; \mathbf{p}; W)$$

and the scattering amplitude on a rotated plane characterized by φ' -rotation in the z axis

$$\mathcal{M}_{\lambda'_1 \lambda'_2, \lambda_1 \lambda_2}^{+, \rho'_2, + \rho_2}(p', \theta', \varphi'; \mathbf{p}; W).$$

Thus, we consider the Lorentz transformation

$$\Lambda = R_{-\varphi', 0, 0} \quad (\text{C1})$$

corresponding to a rotation of an angle φ' around the z axis.

The correspondence between the spinors before and after this Lorentz transformation is

$$S(\Lambda) u_1^\rho(p, \lambda) = \sum_{\lambda'} D_{\lambda' \lambda}(R_\Lambda) u_1^\rho(\Lambda p, \lambda') \quad (\text{C2})$$

$$S(\Lambda) u_2^\rho(p, \lambda) = \sum_{\lambda'} D_{-\lambda', -\lambda}(R_\Lambda) u_2^\rho(\Lambda p, \lambda'), \quad (\text{C3})$$

where $S(\Lambda)$ is the operator that transforms the u, v -states in the Λ Lorentz transformation and D is the usual $D^{1/2}$ Wigner matrix in terms of the rotation angles. The rotation operators are given by

$$R_\Lambda = H_{\Lambda p}^{-1} \Lambda H_p \quad (\text{C4})$$

$$R'_\Lambda = H_{\Lambda p'}^{-1} \Lambda H_{p'}. \quad (\text{C5})$$

In the last equations H_p is the operator that transforms a 4-momentum $(m, \mathbf{0})$ into $p = (E_{\mathbf{p}}, \mathbf{p})$. Details can be found in Ref. [41]. The operation can always be written in a sequence of a boost (L_p) and a rotation ($R_{\mathbf{p}}$)

$$H_p = R_{\mathbf{p}} L_p. \quad (\text{C6})$$

After the Lorentz transformation has been done the following relation between the original and the rotated scattering amplitudes is obtained

$$\begin{aligned} \mathcal{M}_{\alpha'\beta',\alpha\beta}(\Lambda p', \Lambda p; \Lambda P) = \\ \sum_{\substack{\alpha_1, \beta_1 \\ \alpha_2, \beta_2}} S_{\alpha'\alpha_1}(\Lambda) S_{\beta'\beta_1}(\Lambda) \mathcal{M}_{\alpha_1\beta_1, \alpha_2\beta_2}(p', p; P) S_{\alpha_2\alpha}^{-1}(\Lambda) S_{\beta_2\beta}^{-1}(\Lambda). \end{aligned} \quad (\text{C7})$$

for more details see and Appendix B of Ref. [6].

Changing (C7) to the helicity representation according to eq. (3.4) and using the operator rotation properties and the invariance of permutation between boost and rotation operators related to the same axis, we finally conclude that

$$\mathcal{M}_{\lambda'_1\lambda'_2, \lambda_1\lambda_2}^{+\rho'_2, +\rho_2}(p', \theta', \varphi'; p; W) = e^{i\frac{\lambda_1 - \lambda_2}{2}\varphi'} \mathcal{M}_{\lambda'_1\lambda'_2, \lambda_1\lambda_2}^{+\rho'_2, +\rho_2}(p', \theta', 0; p; W). \quad (\text{C8})$$

APPENDIX D: FUNCTION V

In this Appendix we describe how to evaluate V defined by Eq. (4.6). By performing the φ integration we get:

$$V(p', \theta', k, \theta; \bar{\lambda}, W) = \int_0^{2\pi} e^{i\bar{\lambda}\varphi} \bar{\mathcal{V}}(\varphi) d\varphi, \quad (\text{D1})$$

where we use the simplification

$$\bar{\mathcal{V}}(\varphi) = \bar{\mathcal{V}}_{\lambda'_1\lambda'_2, \lambda_3\lambda_4}^{+\rho'_2, +\rho}(p', \theta', 0; k, \theta, \varphi; W). \quad (\text{D2})$$

We note that

$$\bar{\lambda} = \frac{\lambda_1 - \lambda_2}{2}, \quad (\text{D3})$$

so $\bar{\lambda} = 0, \pm 1$.

First, we separate the φ -dependent parts from the independent ones (factorization). Next, we analyze the structure of the resulting functions. We need to consider two different cases: the non vector meson exchange (σ and π) and the vector meson exchange.

1. Factorization of $\bar{\mathcal{V}}(\varphi)$

From the \mathcal{V} expression (see Appendix B) we conclude that

$$\bar{\mathcal{V}}(\varphi) = \delta_I \Lambda_m^4 g_m^2 \bar{V}(\varphi) \mathcal{R}, \quad (\text{D4})$$

where

$$\bar{V}(\varphi) = \frac{[f_{m_i}(q^2)]^2}{\Lambda_m^4} \frac{g_i^2}{\mu^2 - q^2}, \quad (\text{D5})$$

and

$$\mathcal{R} = N_{p'}^2 N_k^2 f_N(p'^2) f_N(k^2) \tilde{H}_i(p', k). \quad (\text{D6})$$

In this equations i is the meson index. Also from Appendix B we have

$$\tilde{H}_i(p', k) = H_i(p', k) Z_1^0 Z_2^0, \quad (\text{D7})$$

for a non vector meson and

$$\tilde{H}_i(p', k) = H_i(p', k), \quad (\text{D8})$$

for vector mesons. Note that the parameterization (D6) is valid for the direct term and for the exchange term if we replace q^2 by \hat{q}^2 , H_i by \widehat{H}_i (and Z_j^0 by \widehat{Z}_j^0 for the non vector case).

Using the coordinates definition (4.1)-(4.3) with $\varphi' = 0$ for q^2 and \hat{q}^2 we can conclude that

$$\bar{V}(\varphi) = \frac{1}{a - b \cos \varphi} \frac{1}{(c - b \cos \varphi)^2}, \quad (\text{D9})$$

where

$$a = \mu^2 + p'^2 + k^2 \mp 2p'k \cos \theta' \cos \theta - q_0^2 \quad (\text{D10})$$

$$b = \pm 2p'k \sin \theta' \sin \theta. \quad (\text{D11})$$

$$c = \Lambda_m^2 + p'^2 + k^2 \mp 2p'k \cos \theta' \cos \theta - q_0^2. \quad (\text{D12})$$

The upper sign should be used in the direct term and the lower sign in the exchange term.

2. \mathcal{R} in terms of φ

The next step is to write \mathcal{R} of eq. (D6) in terms of φ . We need to consider two separate cases: the non vector mesons and the vector mesons.

a. Non vector mesons

For non vector mesons we can write

$$\mathcal{R} = f(\mathbf{p}', \mathbf{k}) \cdot Z_1^0 Z_2^0. \quad (\text{D13})$$

The exact expression of $f(\mathbf{p}', \mathbf{k})$ can be easily deduced from (D6). Attending to the $Z_1^0 Z_2^0$ dependence in φ , we conclude that

$$\mathcal{R} = f(\mathbf{p}', \mathbf{k}) \cdot (c_0 + c_1 e^{-i\lambda_3 \varphi} + c_2 e^{i\lambda_3 \varphi}), \quad (\text{D14})$$

where c_l ($l = 0, \dots, 2$) are known coefficients depending on the scattering conditions and on the helicities states. We can write

$$V(\mathbf{p}', \theta', \mathbf{k}, \theta; \bar{\lambda}, W) = \delta_I \Lambda_m^4 g_m^2 f(\mathbf{p}', \mathbf{k}) \cdot [c_0 \mathcal{F}_0(\bar{\lambda}) + c_1 \mathcal{F}_0(\bar{\lambda} - \lambda_3) + c_2 \mathcal{F}_0(\bar{\lambda} + \lambda_3)], \quad (\text{D15})$$

where the function $\mathcal{F}_0(n)$ is defined as

$$\mathcal{F}_0(n) = \int_0^{2\pi} d\varphi e^{in\varphi} \bar{V}(\varphi), \quad (\text{D16})$$

and n are $n = 0, \pm 1, \pm 2$.

b. Vector mesons

For vector mesons the function \mathcal{R} can be written as a linear combination of the terms

$$Z_1^{\alpha_1} Z_2^{\alpha_2} \quad \text{and} \quad k_i Z_1^{\alpha_1} Z_2^{\alpha_2},$$

where $\alpha_1, \alpha_2 = 0, \dots, 3$. The first term is reduced to the non vector case discussed in subsection D 2 a, because $Z_1^{\alpha_1} Z_2^{\alpha_2}$ can also be written as

$$c_0 + c_1 e^{-i\lambda_3 \varphi} + c_2 e^{i\lambda_3 \varphi},$$

with appropriated coefficients. The second term can be decomposed in 3 cases considered as follows:

Case 1 ($k_1 = k \sin \theta \cos \varphi$)

In this case we need to integrate factors like

$$(k \sin \theta) \cos \varphi e^{in\varphi} \bar{V}(\varphi),$$

and the corresponding term of V , which we label V_1 , is

$$V_1(\mathbf{p}', \theta', \mathbf{k}, \theta; \bar{\lambda}, W) = \delta_I \Lambda_m^4 g_m^2 f(\mathbf{p}', \mathbf{k}) (k \sin \theta) \cdot [c_0 \mathcal{F}_1(\bar{\lambda}) + c_1 \mathcal{F}_1(\bar{\lambda} - \lambda_3) + c_2 \mathcal{F}_1(\bar{\lambda} + \lambda_3)], \quad (\text{D17})$$

where

$$\mathcal{F}_1(n) = \int_0^{2\pi} d\varphi \cos \varphi e^{in\varphi} \bar{V}(\varphi), \quad (\text{D18})$$

with $n = 0, \pm 1 \pm 2$.

Case 2 ($k_2 = k \sin \theta \sin \varphi$)

We have also to consider terms like

$$(k \sin \theta) \sin \varphi e^{in\varphi} \bar{V}(\varphi),$$

from which results for the corresponding V , which we label V_2

$$\begin{aligned} V_2(p', \theta', k, \theta; \bar{\lambda}, W) &= \delta_I \Lambda_m^4 g_m^2 f(p', k) (k \sin \theta) \cdot \\ &[c_0 \mathcal{F}_2(\bar{\lambda}) + c_1 \mathcal{F}_2(\bar{\lambda} - \lambda_3) + c_2 \mathcal{F}_2(\bar{\lambda} + \lambda_3)]. \end{aligned} \quad (\text{D19})$$

The \mathcal{F}_2 function is defined as

$$\mathcal{F}_2(n) = \int_0^{2\pi} d\varphi \sin \varphi e^{in\varphi} \bar{V}(\varphi), \quad (\text{D20})$$

with $n = 0, \pm 1, \pm 2$.

Case 3 ($k_3 = \cos \theta$)

No new φ -dependence appears. This case reduces to the non vector meson case.

3. Functions $\mathcal{F}_l(n)$

The functions $\mathcal{F}_l(n)$ with $l = 0, 1, 2$ can be written in terms of the integrals

$$R_l = \int_0^{2\pi} \bar{V}(\varphi) \cos^l \varphi d\varphi,$$

for $l = 0, \dots, 3$. The R_l integrals are performed analytically with the software program *Mathematica* and simplified afterwards.

REFERENCES

- [1] CLASS Collaboration: R. A. Niyazov, L. B. Weinstein et al. Phys. Rev. Lett. **91**, 252001 (2003).
- [2] J. Adam, Jr., Franz Gross, Sabine Jeschonnek, Paul Ulmer, J. W. Van Orden, Phys. Rev. **C66**, 044003 (2002).
- [3] I. Fachruddin, Ch. Elster, W. Glockle, Phys. Rev. **C68**, 054003 (2003).
- [4] I. Fachruddin, Ch. Elster, W. Glockle, Phys. Rev. **C62**, 044002 (2000); Nucl. Phys. **A689**, 507c (2001).
- [5] Franz Gross, Phys. Rev. **186**, 1448 (1969).
- [6] Franz Gross, J. W. Van Orden and K. Holinde, Phys. Rev. **C45**, 2094 (1992).
- [7] Ch. Elster, J. H. Thomas, W. Glöckle, Few Body Syst. **24**, 55 (1998).
- [8] Ch. Elster, W. Schadow, A. Nogga, W. Glöckle, Few Body Syst. **27**, 83 (1999); W. Schadow, Ch. Elster, W. Glöckle, Few Body Syst. **28**, 15 (2000); H. Liu, Ch. Elster, W. Glöckle, Few Body Syst. **33**, 241 (2003).
- [9] G. Ramalho, A. Arriaga and M. T. Peña, Phys. Rev. **C65**, 034008 (2002).
- [10] B. D. Keister and W. N. Polyzou, Adv. Nucl. Phys. **20**, 225 (1991).
- [11] J. Carlson, V. R. Pandharipande, and R. Schiavilla, Phys. Rev. **C47**, 484 (1993).
- [12] J. L. Forest, V. R. Pandharipande and A. Arriaga, Phys. Rev. **C60**, 014002 (1999).
- [13] Salpeter and Bethe, Phys. Rev. **84**, 1232 (1951).
- [14] R. Blankenbecler and R. Sugar, Phys. Rev. **142**, 1051 (1966).
- [15] V. B. Mandelzweig and Wallace, Phys. Lett **B197**, 469 (1987); S. J. Wallace and V. B. Mandelzweig, Nucl. Phys. **A503**, 673 (1989).
- [16] R. H. Thompson, Phys. Rev. **D1**, 110 (1970).
- [17] K. Erkelenz and K. Holinde, Nucl. Phys. **A194**, 481 (1972).
- [18] Franz Gross, *Relativistic Quantum Mechanics and Field Theory*, Chap. 12, John Wiley & Sons (1993).
- [19] T. Nieuwenhuis and J. A. Tjon, Phys. Rev. Lett. **77**, 814 (1996).
- [20] D. R. Phillips and Stephen J. Wallace, Phys. Rev. **C54**, 507 (1996).
- [21] K. M. Maung and Franz Gross Phys. Rev. **C42**, 1681 (1990).
- [22] G. Ramalho, A. Arriaga and M. T. Peña, Phys. Rev. **C60**, 047001 (1999).
- [23] Alfred Stadler and Franz Gross, Phys. Rev. Lett. **78**, 26 (1997).
- [24] F. Gross, A. Stadler, J. W. Van Orden, N. Devine, Few Body Syst. Suppl. **8**, 269-274,(1995).
- [25] J. Bystricky, F. Lehar and P. Winternitz, J. Phys. (Paris) **39**, 1 (1978).
- [26] G. E. Brown and A. D. Jackson, *The nucleon-nucleon interaction*, North-Holland Publishing Company (1976).
- [27] Franz Gross and D. O. Riska, Phys. Rev. **C36**, 1928 (1987).
- [28] Franz Gross, private communication
- [29] G. Caia, J. W. Durso, Ch. Elster, J. Haidenbauer, A. Sibirtsev and J. Speth, Phys. Rev. **C66**, 044006 (2002).
- [30] G. Ramalho, *Relativistic NN scattering equations without partial wave decomposition*, PhD. thesis (unpublished) (2003).
- [31] George L. Caia, Vladimir Pascalutsa, L. E. Wright, Phys. Rev. **C69**, 034003(2004).
- [32] A. Gersten and Z. Solow, Phys. Rev.**D10**, 1031 (1974).

- [33] **NN-Online:** <http://nn-online.org/NN/>
- [34] J. P. Scanlon *et al.*, Nucl. Phys. **41**, 401, (1963).
- [35] W. Hürster *et al.*, Phys. Lett. B **90**, 367, (1980).
- [36] R. K. Keeler *et al.*, Nucl. Phys. **A377**, 529, (1982).
- [37] T. S. H. Lee and D. O. Riska, Phys. Rev. Lett. **70**, 2237 (1993).
- [38] C. Hanhart, G. A. Miller, F. Myhrer, T. Sato and U. van Kolck, Phys. Rev. **C63** 044002 (2001).
- [39] M. Jacob and G. C. Wick, Ann. Phys. (N.Y.) **7**, 404 (1959).
- [40] G. C. Wick, Ann. Phys. (N.Y.) **18**, 65 (1962).
- [41] Peter A. Carruthers, *Spin and Isospin in Particle Physics Theory*, Chap. 5, Gordon and Breach Science Publishers (1971).

TABLES

m_π	138 MeV
G_π	13.470
λ_π	0.0
Λ_π	1190 MeV
m_σ	497 MeV
G_σ	3.782
m_ρ	770 MeV
G_ρ	0.100
κ_ρ	5.644
m_ω	783 MeV
G_ω	8.100
κ_ω	0.337
Λ_m	2400 MeV
Λ_N	1783 MeV

TABLE I. Model parameters.

I_0	ρ	λ_1	λ_2
1	+	−	−
2	+	−	+
3	+	+	−
4	+	+	+
5	−	−	−
6	−	−	+
7	−	+	−
8	−	+	+

TABLE II. Table defining the indices I_0 , I_k or I' .

Initial state		
	$\lambda = 1$	$\lambda = -1$
$\chi_\lambda(\hat{\mathbf{z}})$	$\begin{pmatrix} 1 \\ 0 \end{pmatrix}$	$\begin{pmatrix} 0 \\ 1 \end{pmatrix}$
$\psi_\lambda(\hat{\mathbf{z}})$	$\begin{pmatrix} 0 \\ 1 \end{pmatrix}$	$\begin{pmatrix} 1 \\ 0 \end{pmatrix}$
Final state		
	$\lambda' = 1$	$\lambda' = -1$
$\chi'_{\lambda'}(\theta, \varphi)$	$\begin{pmatrix} \cos \frac{\theta}{2} e^{-i\frac{\varphi}{2}} \\ \sin \frac{\theta}{2} e^{i\frac{\varphi}{2}} \end{pmatrix}$	$\begin{pmatrix} -\sin \frac{\theta}{2} e^{-i\frac{\varphi}{2}} \\ \cos \frac{\theta}{2} e^{i\frac{\varphi}{2}} \end{pmatrix}$
$\psi'_{\lambda'}(\theta, \varphi)$	$\begin{pmatrix} -\sin \frac{\theta}{2} e^{-i\frac{\varphi}{2}} \\ \cos \frac{\theta}{2} e^{i\frac{\varphi}{2}} \end{pmatrix}$	$\begin{pmatrix} \cos \frac{\theta}{2} e^{-i\frac{\varphi}{2}} \\ \sin \frac{\theta}{2} e^{i\frac{\varphi}{2}} \end{pmatrix}$

TABLE III. Pauli helicity states. The phase differences between these spinors and the ones of these Refs. [39,40] are due to the fact that we consider, for convenience, the rotations convention of Ref. [40] and the phase convention for particle 2 of Ref. [39].

FIGURES

FIG. 1. Helicity representation of the Spectator equation.

FIG. 2. a) Direct term of the kernel $\bar{\mathcal{V}}$. b) Exchange term of the kernel $\bar{\mathcal{V}}$.

FIG. 3. Helicity amplitudes for 300 MeV and partial wave decomposition.

FIG. 4. Helicity amplitudes for 300 MeV and partial wave decomposition.

FIG. 5. Differential cross section results for 99, 200 and 319 MeV.

FIG. 6. Off-mass-shell amplitudes for np process with $\rho = +1$, $\rho' = +1$.

FIG. 7. Off-mass-shell amplitudes for np process with $\rho = +1$, $\rho' = +1$.

FIG. 8. Off-mass-shell amplitudes for np process with $\rho = +1$, $\rho' = -1$.

FIG. 9. Off-mass-shell amplitudes for np process with $\rho = +1$, $\rho' = -1$.

FIG. 10. Partial wave decomposition of the M_3 amplitude for 100, 200 and 300 MeV.

This figure "fig6.gif" is available in "gif" format from:

<http://arxiv.org/ps/nucl-th/0403010v2>

This figure "fig7.gif" is available in "gif" format from:

<http://arxiv.org/ps/nucl-th/0403010v2>

This figure "fig8.gif" is available in "gif" format from:

<http://arxiv.org/ps/nucl-th/0403010v2>

This figure "fig9.gif" is available in "gif" format from:

<http://arxiv.org/ps/nucl-th/0403010v2>

FIGURES

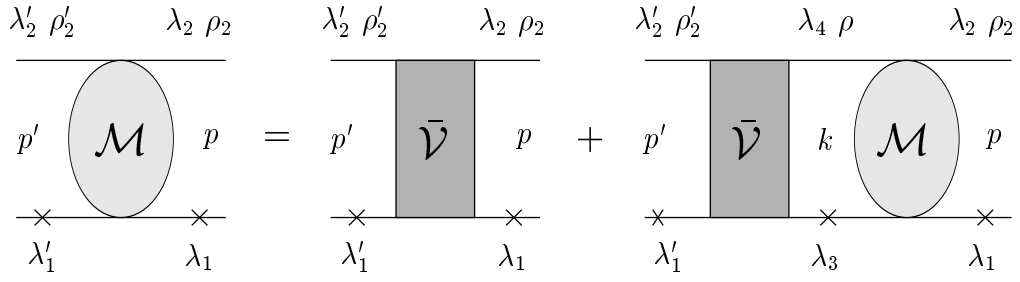


FIG. 1. Helicity representation of the Spectator equation.

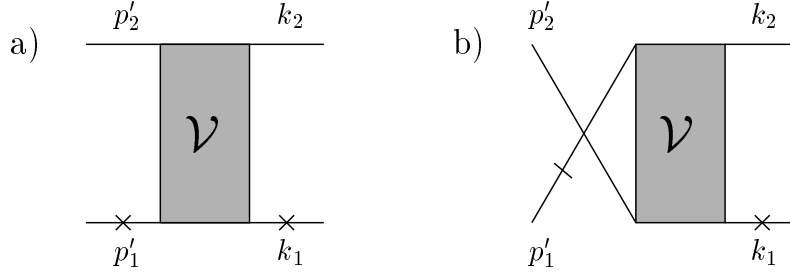


FIG. 2. a) Direct term of the kernel $\bar{\mathcal{V}}$. b) Exchange term of the kernel $\bar{\mathcal{V}}$.

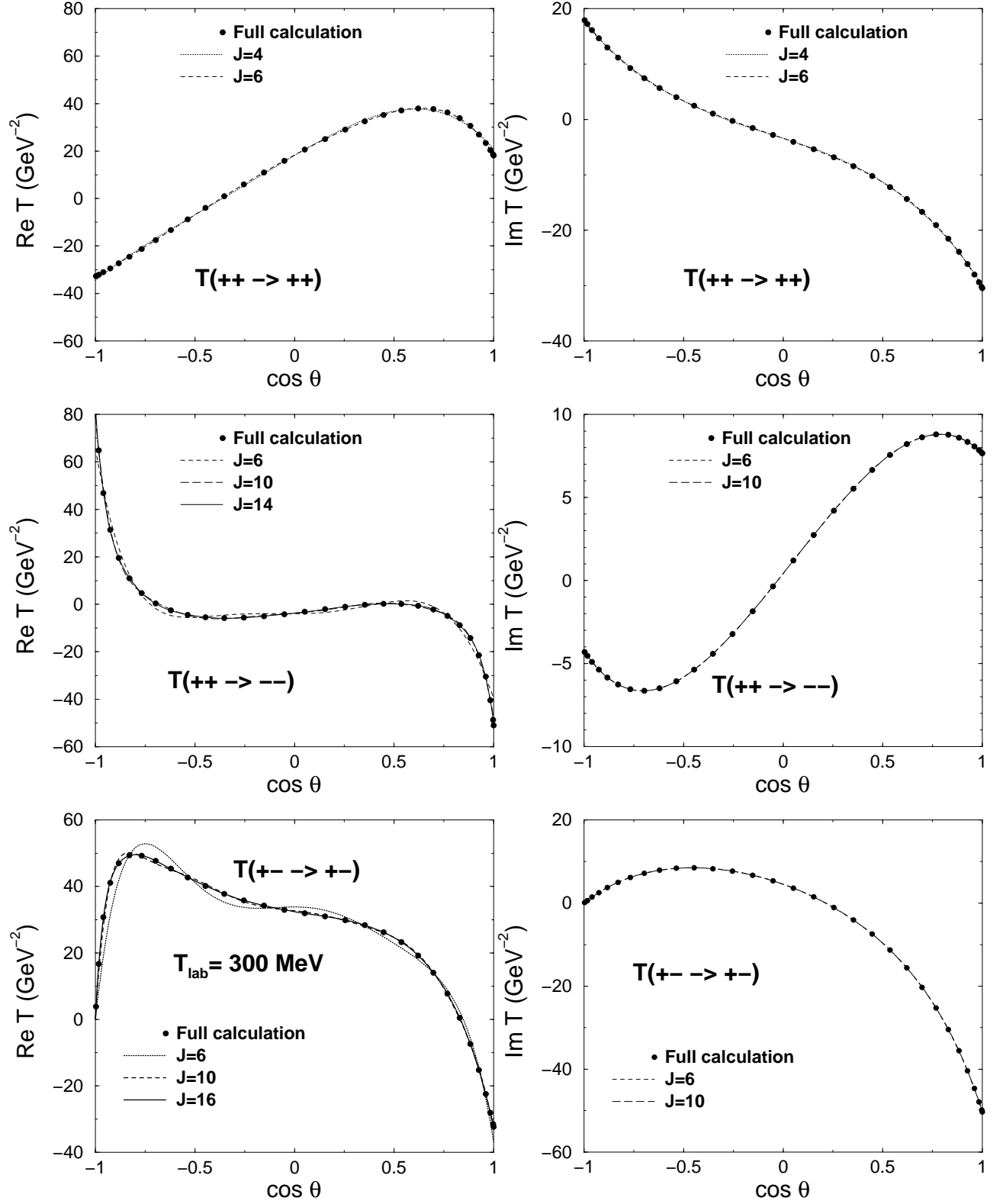


FIG. 3. Helicity amplitudes for 300 MeV and partial wave decomposition.

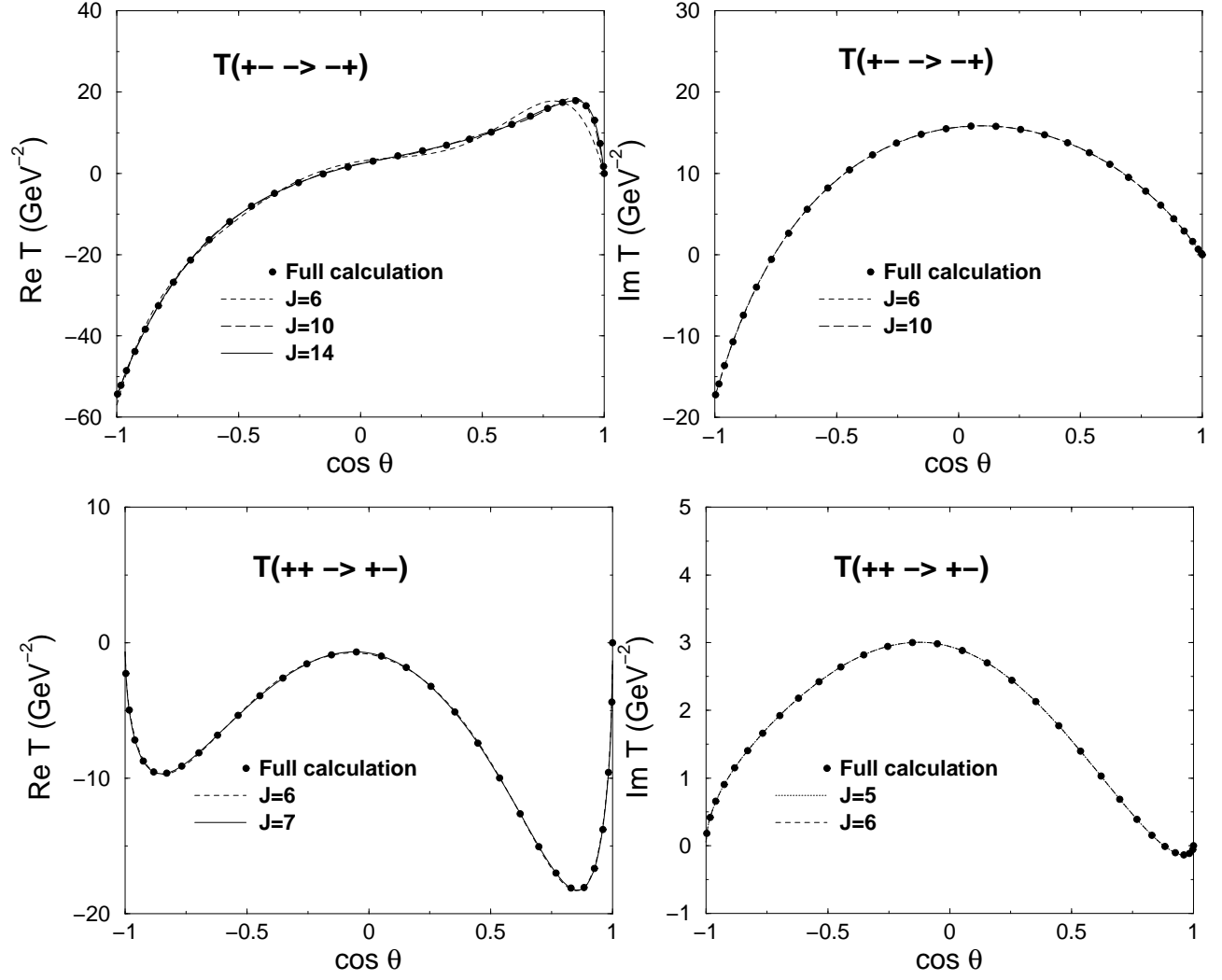


FIG. 4. Helicity amplitudes for 300 MeV and partial wave decomposition.

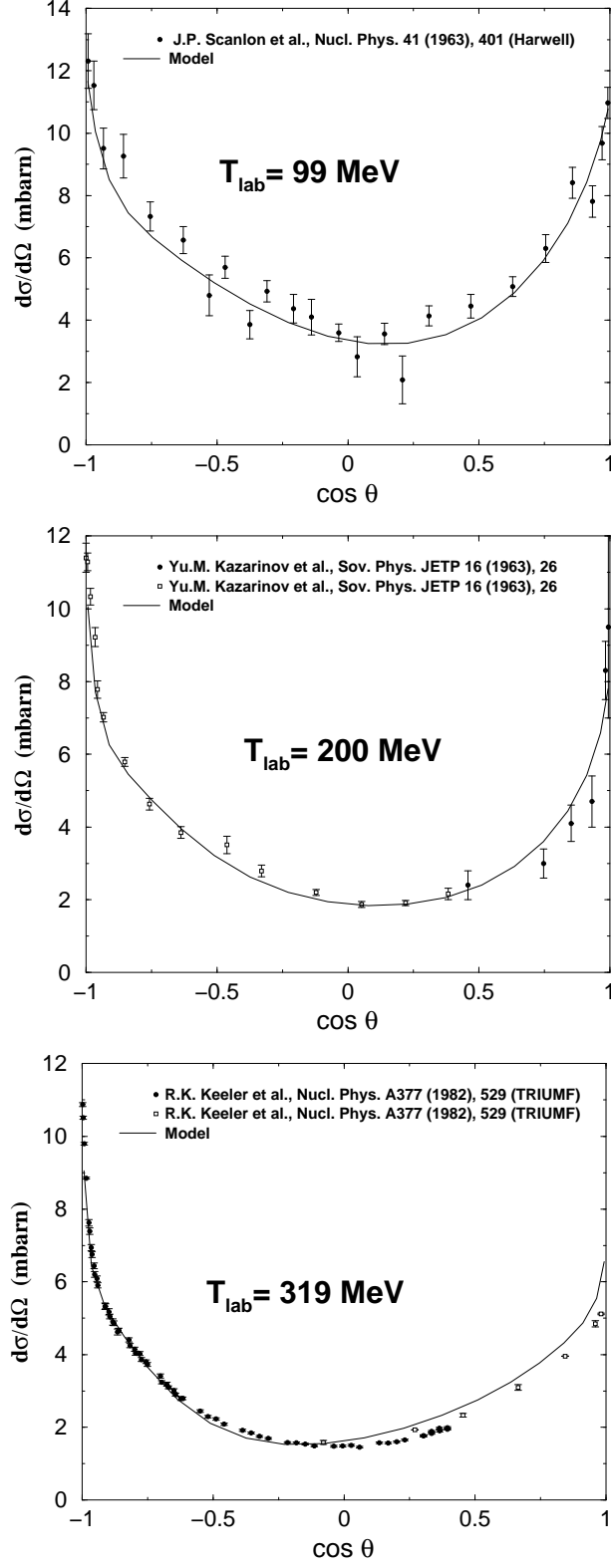


FIG. 5. Differential cross section results for 99, 200 and 319 MeV.

This figure “fig6.gif” is available in ”gif” format.

FIG. 6. Off-mass-shell amplitudes for np process with $\rho = +1$, $\rho' = +1$.

This figure “fig7.gif” is available in ”gif” format.

FIG. 7. Off-mass-shell amplitudes for np process with $\rho = +1$, $\rho' = +1$.

This figure “fig8.gif” is available in ”gif” format.

FIG. 8. Off-mass-shell amplitudes for np process with $\rho = +1$, $\rho' = -1$.

This figure “fig9.gif” is available in ”gif” format.

FIG. 9. Off-mass-shell amplitudes for np process with $\rho = +1$, $\rho' = -1$.

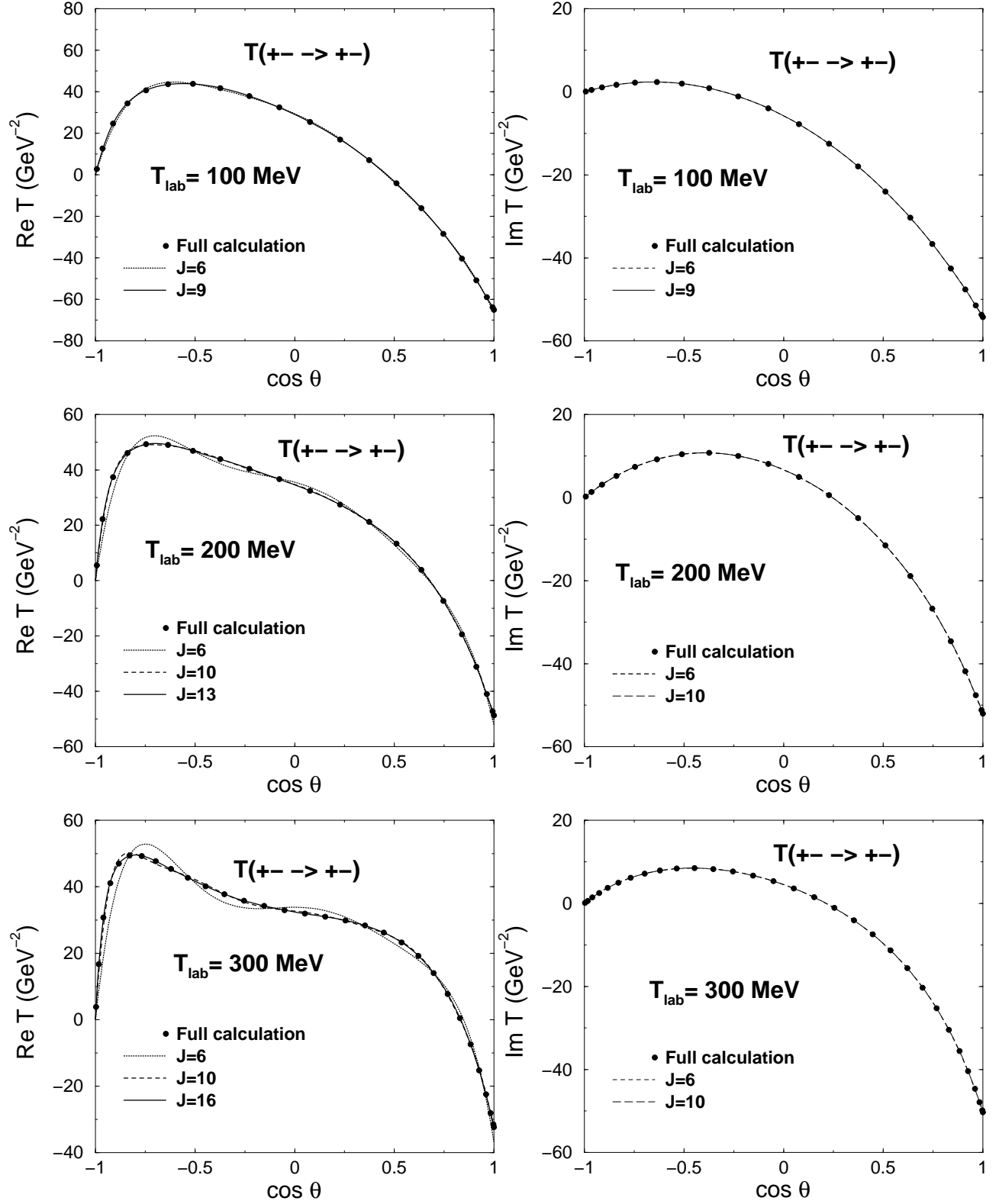


FIG. 10. Partial wave decomposition of the M_3 amplitude for 100, 200 and 300 MeV.